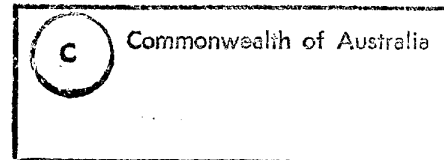
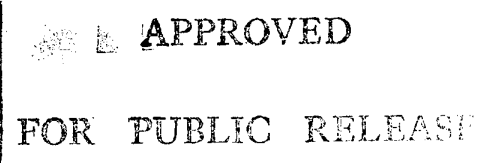


AR-009-242

DSTO-TR-0163

The Performance of Semi-active  
Radar Guided Missiles Against Sea  
Skimming Targets

D. Ciampa and D. Bucco



DTIC QUALITY INSPECTED 5

DEPARTMENT OF DEFENCE  
DEFENCE SCIENCE AND TECHNOLOGY ORGANISATION

19951004 040

# THE PERFORMANCE OF SEMI-ACTIVE RADAR GUIDED MISSILES AGAINST SEA SKIMMING TARGETS

*Dominic Ciampa and Domenic Bucco*

Weapons Systems Division  
Aeronautical and Maritime Research Laboratory

## ABSTRACT

When a radar guided missile engages a target at low altitudes over the sea, the radar signal reflected from the target to the missile may be subject to fading owing to multipath effects. This fading can cause serious missile guidance problems. A radar multipath model has been developed in MATRIXx to evaluate the performance of monopulse semi-active missile systems against low altitude targets. The multipath model takes into account forward scattering over a smooth sea and includes representation of the monopulse sum and difference angle processing performed by the missile receiver. Simulation results, showing the adverse effects of multipath on the seeker boresight errors, are presented for typical missile-to-target engagements.

## RELEASE LIMITATION

*Approved for public release*

DSTO-TR-0163

DEPARTMENT OF DEFENCE

DEFENCE SCIENCE AND TECHNOLOGY ORGANISATION

Accession For	
NTIS GRAIL	<input checked="" type="checkbox"/>
DTIC TAB	<input type="checkbox"/>
Unannounced	<input type="checkbox"/>
Justification	
By	
Distribution	
Availability Codes	
Avail and/or	
Part	Special
A-1	

*Published by*

*DSTO Aeronautical and Maritime Research Laboratory  
GPO Box 1500  
Salisbury South Australia 5108*

*Telephone: (08) 259 5054  
Fax: (08) 259 6090*

*© Commonwealth of Australia 1995  
AR No. 009-242  
April 1995*

### ***Conditions of Release and Disposal***

1. *This document is the property of the Australian Government; the information it contains is released for defence purposes only and must not be disseminated beyond the stated distribution without prior approval.*
2. *The document and the information it contains must be handled in accordance with security regulations applying in the country of lodgement, downgrading instructions must be observed and delimitation is only with the specific approval of the Releasing Authority as given in the Secondary Distribution statement.*
3. *This information may be subject to privately owned rights.*
4. *The officer in possession of this document is responsible for its safe custody. When no longer required this document should be destroyed and the notification sent to: OIC, Corporate Communications Unit, Aeronautical and Maritime Research Laboratory.*

## THE PERFORMANCE OF SEMI-ACTIVE RADAR-GUIDED MISSILES AGAINST SEA SKIMMING TARGETS

### EXECUTIVE SUMMARY

The engagement of a sea skimming target by a radar-guided missile may be subject to multipath effects. That is, the radar signal reflected from the target may return to the missile seeker directly or via reflection from the sea surface giving rise to interference effects. Such interference may cause the target return signal to fade. This multipath-induced fading can cause serious missile guidance problems.

In this report, a radar multipath return model is developed in MATRIXx. This model is used to evaluate the performance of a monopulse semi-active missile system against a sea skimming target. The multipath model takes into account forward scattering over a smooth sea and includes a representation of the monopulse sum and difference angle processing performed by the missile receiver.

A number of parameters affect the return signal from the target. These include the height of the target above the sea surface, the radar cross-section of the target, and the sea state. Simulations were performed for a range of these parameters in order to examine their impact on the target returns and subsequently the missile performance.

The simulation results, which show the adverse effects of multipath on the seeker boresight errors, are presented for typical missile-to-target engagements as a function of the parameters identified above.

The multipath model described here may be used to assess the performance of particular semi-active radar homing missiles when operating over a sea surface.

## Authors

### **Dominic Ciampa** Weapons Systems Division

*Dominic Ciampa is a Research Scientist in WSD. Since joining DSTO in mid-1988 he has been involved in a number of projects which have involved the modelling and simulation of radar guided missiles. These models have been used primarily in the performance evaluation of the terminal effectiveness of the homing guidance of these systems. He has more recently been associated with work for providing post-firing analysis tools for Navy.*

---

### **Domenic Bucco** Weapons System Division

*Domenic Bucco is a Senior Research Scientist in WSD having joined DSTO in 1980 as an Experimental Officer Class 1. In 1983 he was promoted to Research Scientist and worked in the area of autopilot design for gliding munitions. Since 1990, he has been a Senior Research Scientist involved in a number of projects concerned with guidance, control and simulation of radar guided missiles systems with emphasis on developing mathematical models for inclusion in large six degrees of freedom simulation programs for performance assessment of such systems.*

---

## Table of Contents

1. INTRODUCTION . . . . .	1
2. MULTIPATH PROPAGATION . . . . .	1
2.1 Polarisation . . . . .	3
2.2 Efficiency of sea surface reflections . . . . .	3
2.3 Sea state . . . . .	3
2.4 Effect of multipath returns on missile guidance . . . . .	5
3. MODELLING THE ENGAGEMENT . . . . .	6
3.1 Engagement geometry . . . . .	7
3.2 Received signal . . . . .	8
3.3 The antenna gain pattern . . . . .	8
3.4 Generic missile guidance . . . . .	10
3.5 Target model . . . . .	10
3.6 Sea surface reflection characteristics . . . . .	11
3.7 Modelling package . . . . .	11
4. RESULTS AND DISCUSSION . . . . .	12
4.1 Apparent target height . . . . .	14
4.2 Boresight error variations . . . . .	14
4.3 Sea state . . . . .	16
5. CONCLUSIONS . . . . .	16
ACKNOWLEDGMENTS . . . . .	16
REFERENCES . . . . .	18
NOTATION . . . . .	20

## LIST OF FIGURES

1. The multipath engagement scenario for a generic missile against a low altitude target . . . . .	2
2. The reflection coefficient for reflection from the sea surface . . . . .	4
3. The phase angle change on reflection from the sea surface . . . . .	4
4. The variation of the apparent off-boresight angle as a function of the relative phase between direct and indirect target returns as given by equation (5) . . . . .	6
5. The geometry for the multipath engagement scenario . . . . .	7
6. An illustration of the model of the antenna beam pattern adopted . . . . .	9
7. The guidance algorithm modelled including line-of-sight rate reconstruction . . . . .	11
8. SystemBuild block diagram of the multipath model . . . . .	13
9. Apparent target height variations for true heights of 5m, 15m and 30m for sea state zero . . . . .	14
10. The apparent target boresight error (—), the true target boresight error (— — —), and the target image boresight error (---) for target heights of 5m, 15m and 30m and sea state zero . . . . .	15
11. Effect of sea state on the apparent target height . . . . .	17
12. Effect of sea state on the relative power of the returned signal . . . . .	17

## LIST OF TABLES

1. List of superblocks in program structure . . . . .	12
2. Nominal parameters for the simulated engagement . . . . .	13

## NOTATION

$A_d$	Amplitude of the direct return from the target
$A_r$	Amplitude of the reflected return from the target
$A_t$	Amplitude of the signal received by the missile
$G(\epsilon)$	Antenna gain as a function of the off-boresight angle $\epsilon$
$h_m$	Height of the missile
$h_t$	Height of the target
$j$	Imaginary number, $\sqrt{-1}$
$J_1(x)$	Bessel function of the first kind of order 1
$k$	Navigation Ratio or PN gain
$K$	Slope of the monopulse error curve
$N'$	Effective guidance gain
$N_c$	Called for acceleration
$R$	Range from the target to the missile
$R_1$	Range from the target to the reflecting surface
$R_2$	Range from the reflecting surface to the missile
$t$	Time
$T_a$	Autopilot time constant
$T_s$	Seeker gyro time constant
$V_c$	Closing velocity
$x$	Variable
$\Delta$	Difference voltage gain
$\epsilon$	Sea dielectric constant
$\epsilon_c$	Complex dielectric constant
$\epsilon_i$	Boresight angle to the target image
$\epsilon_m$	Boresight angle to the apparent target
$\epsilon_t$	Boresight angle to the target
$\dot{\gamma}$	Turning rate of the missile flight path
$\Gamma$	Smooth sea reflection coefficient
$\lambda$	Radar wavelength
$\theta_i$	Inertial angle to the target image from the missile
$\theta_s$	Pointing angle of the seeker head in inertial axes
$\theta_t$	Inertial angle to the target from the missile
$\phi$	Sum of the phase angles of the direct and image returns
$\phi_d$	Phase of the direct return from the target
$\phi_r$	Phase of the image return from the target
$\phi_t$	Phase of the signal received by the missile
$\Delta\phi(\psi)$	Phase change on reflection for incidence angle $\psi$
$\rho$	Ratio of the amplitude of the image signal to the target signal at the missile
$\rho_c$	Coherent scattering co-efficient
$\rho_{ss}$	$\rho$ modified to account for the effect of sea state

$\rho_1$	Ratio of image to target amplitudes before reflection of the image signal
$\rho_2$	Magnitude of the Fresnel reflection co-efficient
$\sigma$	Sea conductivity
$\sigma_A$	RCS of target as viewed by the missile from a positive aspect angle
$\sigma_B$	RCS of target as viewed by the missile from a negative aspect angle
$\dot{\sigma}$	Turning rate of missile-to-target line-of-sight rate
$\hat{\dot{\sigma}}$	Reconstructed missile-to-target line-of-sight rate
$\Sigma$	Sum voltage gain
$\omega$	Angular frequency of the illuminating radar
$\psi$	Grazing or incidence angle

## 1. INTRODUCTION

The purpose of this report is to examine the performance of a generic radar-guided missile, with a monopulse receiver, against low-altitude targets flying over the sea surface. It has been shown that signal fading due to the multipath interference can cause serious guidance problems for the monopulse tracker [1,2]. In respect to a semi-active missile, these guidance problems may arise from the multipath returns along any one of the three radar pathways possible in this type of scenario. These pathways are: 1) the transmit path from the illuminator to the missile rear receiver, 2) the transmit path from the illuminator to the target, and 3) the receive path from the target to the missile front receiver. Within each of these three distinct pathways, there are two possible forward paths that the transmitted signals may take, namely, a direct path and via reflection from the sea surface. The multipath model presented here is based on consideration of the latter pathway only (see Figure 1). Other multipath-affected pathways likely to pose serious guidance problems for a semi-active seeker will be considered in future studies.

The modelling approach taken was twofold. Firstly, a multipath model which adequately represents the reflection characteristics of the sea surface was developed and implemented in MATRIXx. The model assumes a flat earth geometry with smooth sea surface conditions, that is, zero sea state. Extensions to higher sea states were modelled according to Ament's theory on specular reflection [4]. However, no modelling of the diffuse components of the sea surface reflections was considered [3]. The monopulse seeker processing was included in the model as well as attenuation effects due to the sum and difference voltage gain patterns associated with the seeker antenna. This provides valuable insight into the way the seeker processes the multipath affected signal and calculates the off-boresight angle to the target.

Secondly, a pitch plane engagement model utilising the multipath affected returns from the target was developed and implemented in MATRIXx. Only multipath effects in the vertical plane were considered. The target is assumed to be non-maneuvring and travelling at constant speed and height. It is further assumed that the missile follows a proportional navigation guidance law and travels at a constant speed.

The structure of the report is as follows. Section 2 discusses multipath propagation in general, and identifies factors that influence the effect, particularly in reference to the reflection characteristics of the sea surface. Section 3 describes the model used to quantify multipath propagation contamination of homing signals in a semi-active radar guided missile. Section 4 presents and discusses the results obtained with the model. Finally, a brief summary of the report conclusions is given and the direction of future investigations indicated.

## 2. MULTIPATH PROPAGATION

The propagation of radar signals between a source (the illuminator), a target, and a receiver (which may or may not be co-located with the illuminator), is influenced by several factors. These factors include atmospheric effects such as attenuation and multipath propagation. The latter effect is the only one discussed here.

Multipath is defined as the propagation of electromagnetic waves emanating from one point and arriving at another via different paths. In the case of radar propagation, effects due to multipath occur when two or more electromagnetic waves emanating from a single source, propagate along different paths to the same receiver.

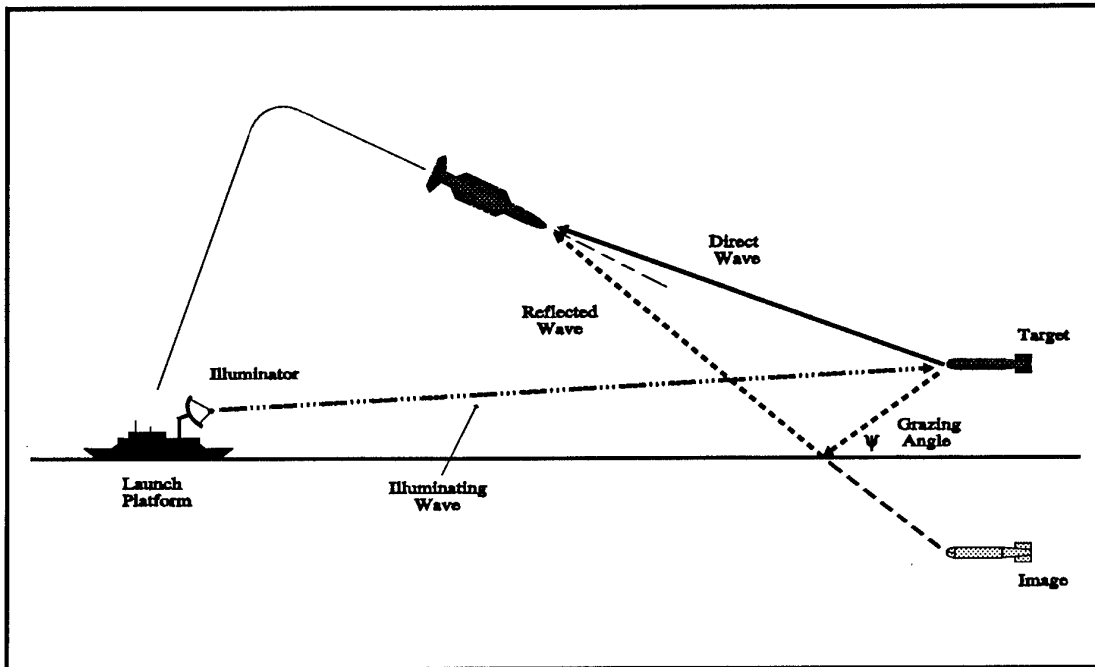


**Figure 1** The multipath engagement scenario for a generic missile against a low altitude target

Any study of the multipath effects on a semi-active radar guidance system must first recognise that this involves a bistatic radar wherein the transmitter is on the launch platform (a ship) and the receiver is in an airborne missile. This gives rise to differences in the possible propagation paths, target cross section, doppler shifts, and glint, as compared to a monostatic radar wherein the transmitter and receiver are co-located [1]. For example, consider the multipath scenario depicted in Figure 1. When the target is illuminated by the shipboard tracking radar, the direct reflection of this illumination from the target to the missile occurs from a positive aspect angle relative to the illumination axis and thus has a different effective radar cross section (RCS) than that seen by the target illuminator. Another target reflection which propagates toward the sea surface occurs from a negative aspect angle with respect to the illumination axis. This effective cross section is usually different from that of the direct path and can even be larger for targets which have more radar-reflective lower structures. The bistatic differences in glint and doppler shifts arise from these same differences in the aspect angles for the direct and reflected paths versus the illumination axis [1].

The strength of the sea surface reflected signal depends on several factors. These include the efficiency of the reflection process (wavelength and sea state dependent) and the polarisation of the incident radiation. Many systems operate at X-band, hence a wavelength of 3 cm (10 GHz) was adopted. The effect of these parameters is briefly indicated below (sections 2.1 to 2.3), as well as a discussion of the qualitative effects of multipath returns on missile guidance (section 2.4).

## 2.1 Polarisation

In order to minimise multipath effects, many semi-active radar systems use vertical polarisation. This is because horizontally polarised radar at X-band is reflected far more efficiently from a flat surface than vertically polarised radar. Hence the latter is likely to result in significantly weaker multipath signals.

## 2.2 Smooth sea reflection coefficient

The efficiency of the reflection process is dependent on the *grazing angle*,  $\psi$ , the angle between the incident radiation and the reflecting surface, as illustrated in Figure 1. On reflection from the sea-surface, the negative aspect angle wave will suffer both attenuation and a phase change. For vertical polarisation, this attenuation in magnitude and attendant phase change is described by the smooth sea reflection coefficient, also known as the Fresnel reflection coefficient [4], namely:

$$\Gamma = \frac{\epsilon_c \sin \psi - \sqrt{\epsilon_c - \cos^2 \psi}}{\epsilon_c \sin \psi + \sqrt{\epsilon_c - \cos^2 \psi}} \quad (1)$$

where the complex dielectric constant  $\epsilon_c$  appearing in the above expression is approximated by

$$\epsilon_c = \epsilon - j60\lambda\sigma, \quad (2)$$

and  $\epsilon$  is the sea dielectric constant,  $\lambda$  is the radar wavelength (m) and  $\sigma$  is the sea conductivity (mho/m).

The magnitude of this reflection coefficient as a function of grazing angle has been calculated for typical sea water properties and reproduced as Figure 2. The corresponding phase for similar grazing angles has been depicted in Figure 3. From Figure 2, it is clear that, at the so-called 'Brewster angle', the reflection of vertically polarised radar at X-band is significantly reduced and consequently the indirect or reflected wave will be attenuated far more than at other angles.

## 2.3 Sea state

Reflection from the sea surface may be specular or diffuse, or a combination. Specular reflection occurs from a surface which is flat and very smooth. If the surface is irregular, the multipath is called diffuse. In the case where the surface is smooth, but is perturbed by small scale irregularities, both specular and diffuse multipath are present, producing, in effect, coherent and incoherent components respectively. For the purpose of this report, only the specular multipath return is considered. This corresponds to ideal conditions in which the sea surface is very smooth and is generally designated as sea state zero. The effects of the diffuse components are discussed in [3].

In the case being considered here, with low-altitude targets approaching at shallow angles over the reflecting surface of the sea, there may not be enough separation in angle, range, or doppler to resolve the direct and reflected waves from the target. As the multipath is specular, this will represent a situation equivalent to a number of unresolved targets, which are related according to the geometry and electrical characteristics of the reflecting surface. This will cause a major problem for the guidance of the missile as the apparent target position will vary with time with the variation in the direct and reflected signals.

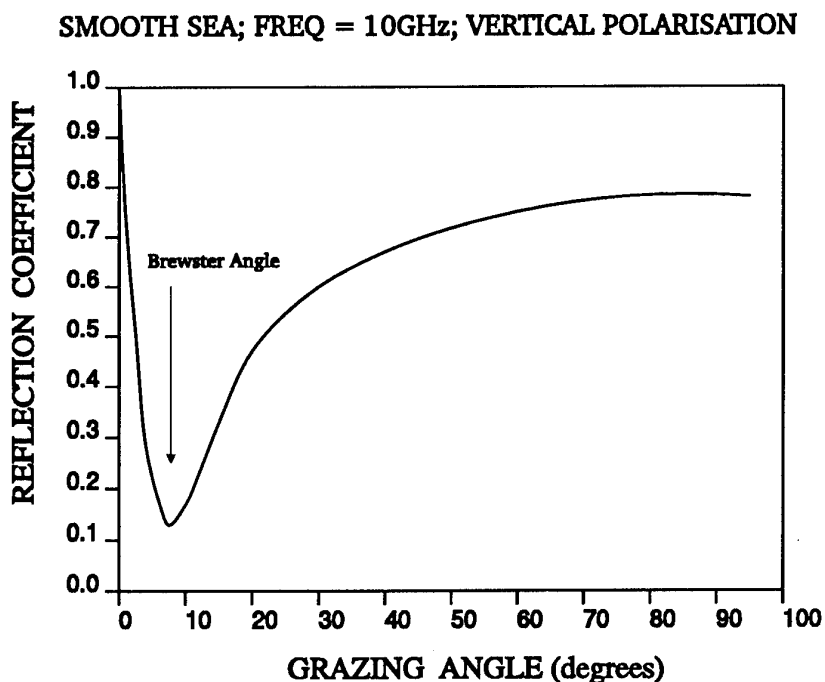


**Figure 2** The reflection coefficient for reflection from the sea surface

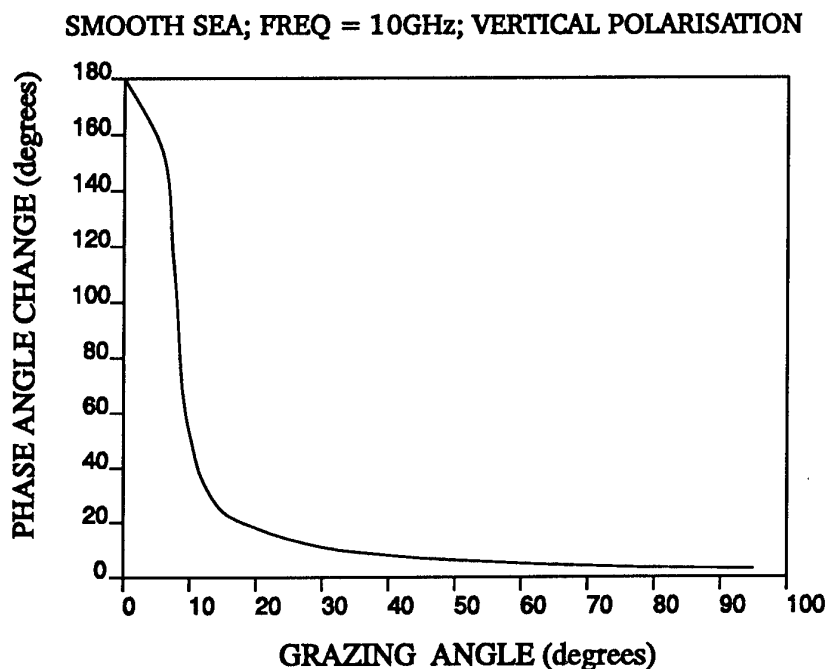


**Figure 3** The phase angle change on reflection from the sea surface

## 2.4 Effect of multipath returns on missile guidance

The signal received at the missile is processed to determine its direction of origin. In the presence of multipath, this signal is a combination of the direct target skin return and a return seemingly emanating from the target image beneath the sea surface. With a monopulse receiver, the sum and difference voltages generated by this composite signal are electronically manipulated to obtain the off-boresight angle to the target, that is, the angle between the pointing direction and the 'apparent' direction to the target. This angle, denoted here by  $\epsilon_m$ , is processed to provide appropriate guidance signals for the missile.

From Sherman [5], the indicated angle to the apparent target is proportional to the ratio of difference and sum voltage gains and is given by:

$$\epsilon_m = K Re \left( \frac{\Delta}{\Sigma} \right), \quad (3)$$

where  $K$  refers to the slope of the monopulse response curve versus off-boresight angle and  $\Delta, \Sigma$  denote the difference and sum voltages, respectively.

It can be shown that for the case under consideration here,  $\epsilon_m$  is well represented by [5]:

$$\epsilon_m = \frac{\epsilon_t + \rho(\epsilon_t + \epsilon_i) \cos \phi + \rho^2 \epsilon_i}{1 + 2\rho \cos \phi + \rho^2} \quad (4)$$

where  $\epsilon_t$  and  $\epsilon_i$  are the off-boresight angles to the target and image respectively,  $\phi$  is the sum of phase angles of the direct,  $\phi_d$ , and reflected,  $\phi_r$ , returns, that is:

$$\phi = \phi_d + \phi_r$$

and  $\rho$  is the ratio of the amplitude of the image signal with respect to the target signal (see section 3.3).

The behaviour predicted by this equation is examined in the following where the open loop case is considered, that is, the seeker head remains fixed and only the open loop indicated angle (relative to the seeker boresight) varies as a result of changes in the relative phase, amplitude ratio, and/or angular locations of the target. In this case it is assumed that

$$\epsilon_i = -\epsilon_t$$

and therefore equation (4) reduces to

$$\frac{\epsilon_m}{\epsilon_t} = \frac{1 - \rho^2}{1 + 2\rho \cos \phi + \rho^2} \quad (5)$$

Equation (5) is represented graphically in Figure 4 for a range of indicative values of  $\rho$  from 0.1 through to 5.

Figure 4 shows that the apparent line-of-sight to the target can be quite large, especially at relative phase angles near  $180^\circ$ , as well as being a periodic function of the relative phase between

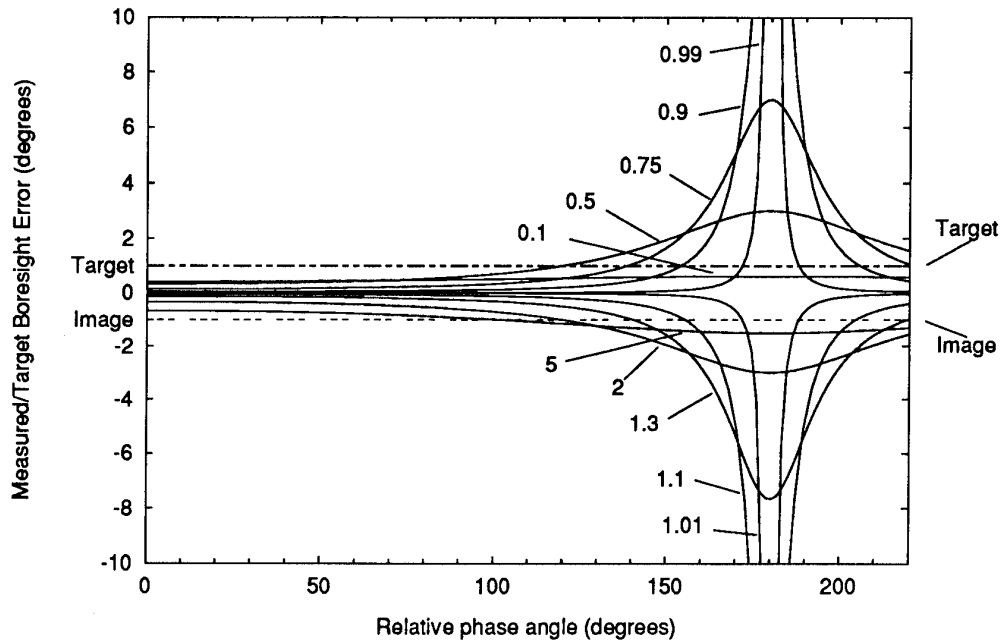


**Figure 4** The variation of the apparent off-boresight angle as a function of the relative phase between direct and indirect target returns as given by equation (5)

the returned signals. Furthermore, for values of  $\rho < 1$ , the apparent target always lies above the sea surface (defined by  $\epsilon_m/\epsilon_t = 0$ ), and conversely, for  $\rho > 1$ , the apparent target lies below the sea surface. For  $\rho$  near 1, the apparent target lies near the sea surface except for relative phases near  $180^\circ$ . This latter point indicates that if  $\rho$  is varying about unity, then the angular error,  $\epsilon_m$ , can fluctuate wildly between two extremes which extend beyond the angle between the target and image. However, because of the relatively long seeker time constant and high closing velocities associated with a missile engagement, this is a transient situation which should cause little degradation of the missile performance.

It should be noted that this was for an open loop response. In the closed loop case which applies here (see Figure 7), the seeker attempts to null the angle error  $\epsilon_m$ , this having the effect of varying  $\rho$ , thereby making the analysis more complicated [5]. However, the simpler open loop response has been used to indicate qualitatively the factors which will affect missile guidance in a multipath situation.

### 3. MODELLING THE ENGAGEMENT

In this section, the components of the model are discussed. These components include the engagement geometry, the model of the receiving antenna, the guidance law, the reflection characteristics of the sea surface, and the target model. Finally, the modelling package used for these investigations is discussed including a break down of the major sections of the model.

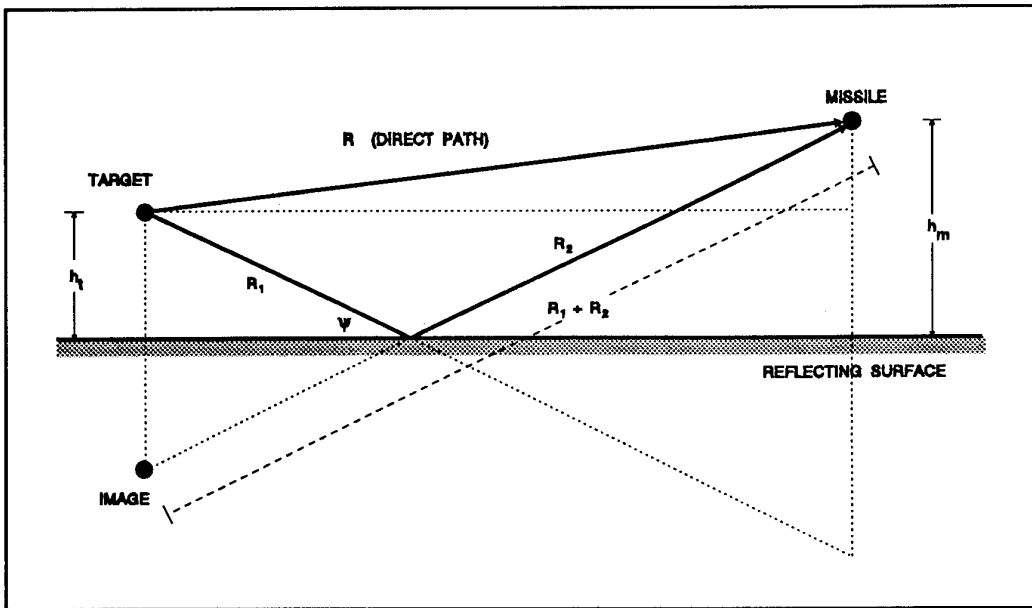


**Figure 5** The geometry for the multipath engagement scenario

### 3.1 Engagement geometry

To simplify the discussion which follows, a flat-earth geometry is assumed. The geometry for the engagement under consideration is shown in Figure 5. The grazing angle of the reflected wave,  $\psi$ , will have a major bearing on the reflection coefficient and phase angle change on reflection from the sea surface (see Figures 2 and 3). This angle can be determined from the geometry to be given by:

$$\tan \psi = \sqrt{\frac{(h_m + h_t)^2}{R^2 - (h_m - h_t)^2}} \quad (6)$$

where  $h_t$  and  $h_m$  are the heights of the target and missile respectively, and  $R$  is the length of the direct path between the target and missile. It can be similarly shown that the length of the reflected path,  $R_1 + R_2$ , is given by:

$$R_1 + R_2 = \frac{h_m + h_t}{\sin \psi} \quad (7)$$

The phase of the signal incident at the receiver is an important quantity for reconstructing the direction of arrival of the return. From the geometry, the phase of the direct return from the target,  $\phi_d$ , is given by:

$$\phi_d = \frac{2\pi R}{\lambda} \quad (8)$$

and the phase of the return from the sea surface,  $\phi_r$ , will be:

$$\phi_r = \frac{2\pi(R_1 + R_2)}{\lambda} + \Delta\phi(\psi) \quad (9)$$

where  $\lambda$  is the wavelength of the illuminating radar and  $\Delta\phi(\psi)$  is the phase change on reflection for incidence angle  $\psi$ .

### 3.2 Received signal

If we consider, in general, the direct return to have an amplitude  $A_d$  and phase  $\phi_d$ , and the indirect return to have an amplitude  $A_r$  and phase  $\phi_r$ , then the two signals can be represented by the time varying phasors

$$A_d \sin(\omega t + \phi_d)$$

and

$$A_r \sin(\omega t + \phi_r)$$

Therefore, the total received signal will be:

$$A_t \sin(\omega t + \phi_t) = A_d \sin(\omega t + \phi_d) + A_r \sin(\omega t + \phi_r) \quad (10)$$

where  $A_t$  and  $\phi_t$  are the amplitude and phase of the total received signal. Expanding this equation and equating terms gives:

$$A_t \sin \phi_t = A_d \sin \phi_d + A_r \sin \phi_r$$

and

$$A_t \cos \phi_t = A_d \cos \phi_d + A_r \cos \phi_r$$

Then in terms of the direct and indirect signals, the received signal will be characterised by an amplitude and phase given by:

$$A_t^2 = (A_d \sin \phi_d + A_r \sin \phi_r)^2 + (A_d \cos \phi_d + A_r \cos \phi_r)^2 \quad (11)$$

and

$$\tan \phi_t = \frac{A_d \sin \phi_d + A_r \sin \phi_r}{A_d \cos \phi_d + A_r \cos \phi_r} \quad (12)$$

### 3.3 The antenna gain pattern

The receiving antenna has a gain which is dependent on the angle to the boresight at which the incident radiation arrives, the off-boresight angle,  $\epsilon$ . For a generic monopulse antenna pattern, the gain function of the voltage sum pattern,  $G(\epsilon)$ , may be well-described by the following expression:

$$G(\epsilon) = \frac{2J_1(x)}{x} \quad (13)$$

where  $J_1(x)$  is a Bessel function of the first kind of order one. The gain function, as represented by this expression with  $x = 9\pi\epsilon$  is illustrated in Figure 6.

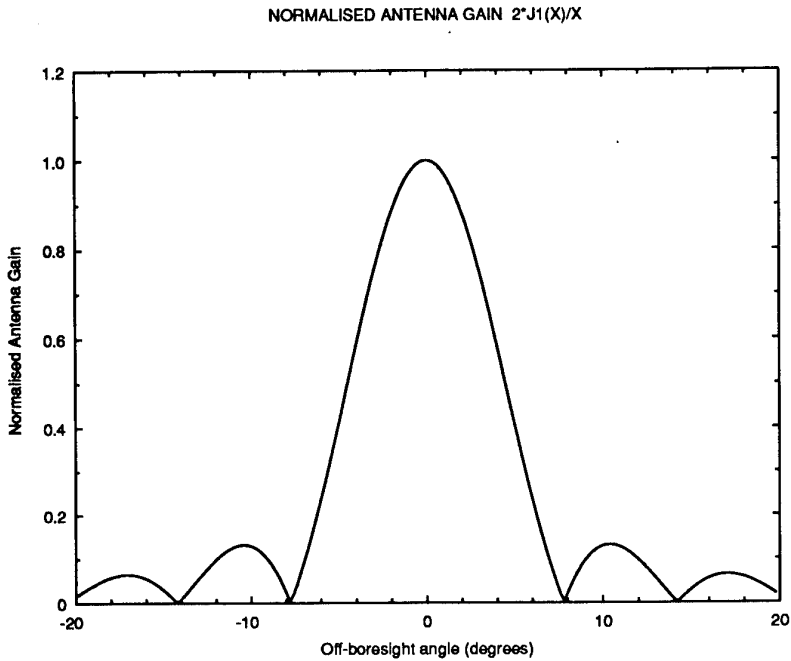


**Figure 6** An illustration of the model of the antenna beam pattern adopted

The gain of the antenna will act to attenuate the signal strength entering the receiver. If  $G(\epsilon_t)$  and  $G(\epsilon_i)$  are the antenna gains in the direction of the target and image respectively, then the relative amplitude of the image signal with respect to that of the target,  $\rho$ , is given by:

$$\rho = \rho_1 \rho_2(\psi) \frac{G(\epsilon_i)}{G(\epsilon_t)} \quad (14)$$

where

$\rho_1$  is the ratio of radar cross sections of the image and target reflecting surfaces as viewed by the missile receiver, and

$\rho_2$  is the magnitude of the Fresnel reflection coefficient dependent on the grazing angle  $\psi$  as given by equation (1).

If we consider  $\phi_d = 0$  as our reference phase, and  $\rho$  to be the ratio of signal amplitudes of the image to target as defined by equation (14), then equations (11) and (12) can be rewritten as

$$\left( \frac{A_t}{A_d} \right)^2 = 1 + \rho^2 + 2\rho \cos \phi \quad (15)$$

where  $\phi = \phi_d + \phi_r$ , and

$$\tan \phi_t = \frac{\rho \sin \phi}{1 + \rho \cos \phi} \quad (16)$$

Equations (15) and (16) can be used to calculate the phase and amplitude of the total received signal from the target.

### 3.4 Generic missile guidance

A basic pitch plane trajectory model is used for the missile. A brief description of the model follows.

The inertial angles relating the angular positions of the target,  $\theta_t$ , the image,  $\theta_i$ , and the pointing direction of the seeker head,  $\theta_s$ , are used to determine the off-boresight angles to the target and image,  $\epsilon_t$  and  $\epsilon_i$ . These are used with the received signal represented by  $\rho$  and  $\phi$ , and processed in accordance with equation (4) to determine the apparent boresight error  $\epsilon_m$ . This is then used for missile guidance based on a proportional navigation (PN) guidance algorithm. In this case, the turning rate of the missile,  $\dot{\gamma}$ , is proportional to the turning rate of the missile-to-target line-of-sight (LOS),  $\dot{\sigma}$ , that is:

$$\dot{\gamma} = k \dot{\sigma} \quad (17)$$

where  $k$  is the proportionality constant called the navigation ratio, or PN gain.

The line-of-sight rate is generated by the seeker head tracking the target and attempting to keep the target on boresight. Any off-boresight deviation,  $\epsilon_m$ , results in a demand to move the seeker head to null the deviation. The off-boresight angle is used to reconstruct the line-of-sight rate,  $\dot{\sigma}$ , using the algorithm illustrated by Figure 7, where the seeker boresight error is combined with the integrated rate gyro signal (see reference [6]). The response of the seeker gyro is modelled as a first order lag with a time constant  $T_s$ .

The line-of-sight rate is then used to demand the called-for-acceleration,  $N_c$  (or  $A_{dem}$  in Figure 7), given by:

$$N_c = N' \dot{\sigma} V_c \quad (18)$$

where  $V_c$  is the relative closing velocity between the missile and the target, and  $N'$  is the effective guidance gain with a value in the range 2–5. A value of 4 is adopted here. This demand, with g-bias, is fed to the autopilot which is assumed to respond as a first order lag with a time constant of  $T_a$ , resulting in the achieved acceleration.

### 3.5 Target model

The target model adopted in these preliminary investigations is of a non-manoeuvring target travelling at constant speed and at a constant altitude. The ratio of the target radar cross section (RCS) between the positive and negative aspect angles is assumed to be a variable input. In this context, the positive aspect angle is defined as the angle from the illuminator beam to the target echo towards the missile measured in a clockwise direction (see Figure 1). Likewise, the negative aspect angle is defined as the angle from the illuminator beam to the target echo towards the sea surface and measured in a counterclockwise direction.

Consequently, the RCS Ratio is defined, as given in reference [7], in terms of the target's average radar cross section in the direction of the line-of-sight of the missile,  $\sigma_A$ , and its average radar cross section in the direction of the specular reflection point on the sea surface,  $\sigma_B$ , that is:

$$\text{RCS Ratio} = 10 \log \left( \frac{\sigma_A}{\sigma_B} \right). \quad (19)$$

In addition, as mentioned previously, the simulation program has the facility to accommodate the target's bistatic RCS profile, should such information be known for a specific target.

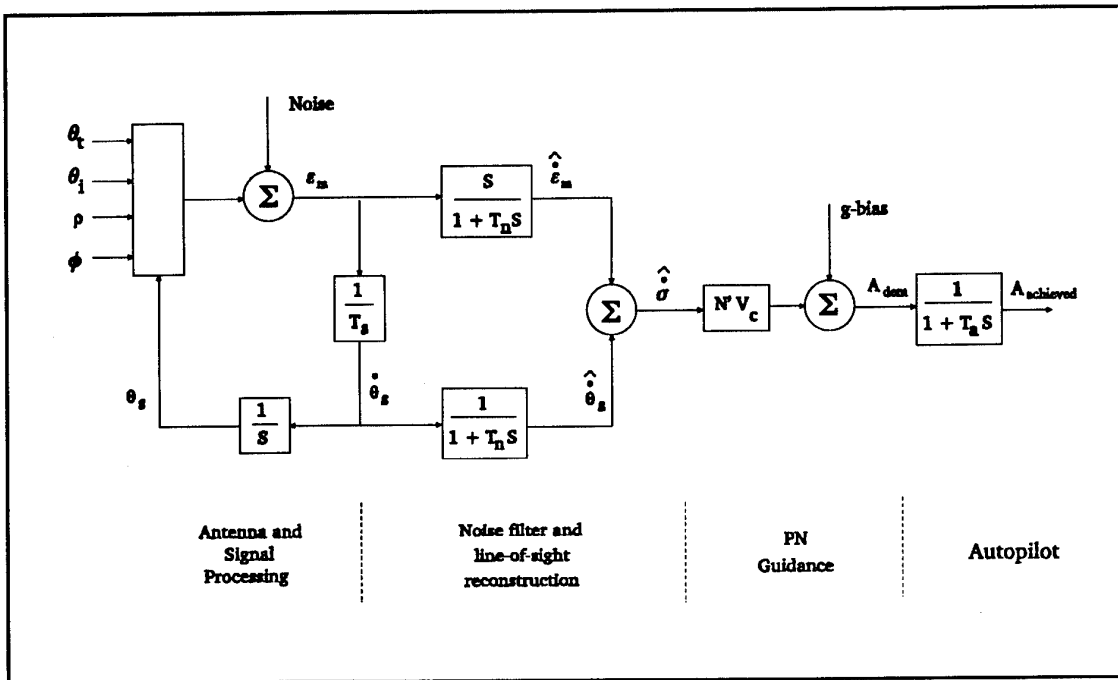


**Figure 7** The guidance algorithm modelled including line-of-sight reconstruction

### 3.6 Sea surface reflection characteristics

The properties associated with the reflection of radar waves by the sea surface are dependent on the angle of incidence of the radiation, its polarisation, and the sea state. In the case considered here of vertical polarisation and a flat sea surface, the attenuation and phase change on reflection as a function of the grazing angle are as given in Figures 2 and 3.

### 3.7 Modelling package

The model is developed using the MATRIXx<sup>R</sup> simulation package. MATRIXx is a powerful, programmable, matrix calculator which offers a graphics capability. Within MATRIXx the user is able to access the SystemBuild<sup>R</sup> environment where block diagrams are generated and the simulation environment provided.

The MATRIXx model to represent the effects of multipath interference is represented in Figure 8 by its SystemBuild block diagram. This shows the different blocks which make up the flow of the model. There are six main 'Superblocks' which essentially equate to functions or subroutines in other programming languages. There are also some superblocks within these superblocks. The complete listing is not given, but the calculations performed by each superblock are described in Table 1. The multipath model is part of the overall engagement model and uses the position of the missile (XM,ZM) and the position of the target (XT,ZT) to determine the 'apparent position' of the target in the presence of multipath returns. This apparent position is used by the missile model (Figure 7) to generate guidance commands. This will allow an assessment of the response of the missile to target position fluctuations which occur in an environment where multiple returns from a target are possible. This is examined in the following section.

**Table 1** List of superblocks in program structure

Superblock	Function
Flat Earth Geometry	In this superblock, the geometrical parameters of the engagement are calculated. This includes the range of the missile to the target and image, and the lookdown angles to the target and image relative to the missile centerline.
Reflection Coefficient	This superblock determines the coefficients for amplitude attenuation and phase change of the target signal reflected from the sea surface along the line-of-sight to the missile receiver.
Monopulse Processor	The superblock determines the off-boresight angles to the target ( $\epsilon_{st}$ ) and the target image ( $\epsilon_{si}$ ) from the geometry, and the off-boresight angle to the apparent target ( $\epsilon_{sm}$ ) using phase monopulse techniques to process the multipath signals received by the missile from the 'target'.
LOS Rate Reconstruction	Using the boresight error to the 'apparent target', the line-of-sight rate is calculated assuming a seeker head time constant of 0.2 seconds.
Seeker Head Angle	In this superblock, the seeker head angle is determined from the seeker head rate and line-of-sight rate.
Apparent Target Height	Calculates the apparent target position from the signal received by the missile receiver. This uses the apparent target position, the seeker head angle and the position of the missile relative to the true target position.

#### 4. RESULTS AND DISCUSSION

The engagement model was run for a scenario chosen as representative of the final stages of a typical low-altitude target engagement. The important quantities to be extracted from the simulation include those factors that are indicative of missile performance. For the multipath environment case, a significant factor affecting missile performance is the apparent target position - the target position as seen by the seeker - since missile guidance ultimately depends on this.

The nominal parameters of the engagement scenario considered in this analysis are given in Table 2. It should be noted here that the scenario is assumed to begin in the terminal phase of the engagement, therefore initial parameters relate to the beginning of this phase, not missile launch conditions.

For the initial conditions given in Table 2, several cases of target height and sea state have been considered. Target heights of 5m, 15m and 30m have been chosen for simulation purposes as well as sea states of zero and three. The effect of sea state is represented by replacing  $\rho$  in equation (14)

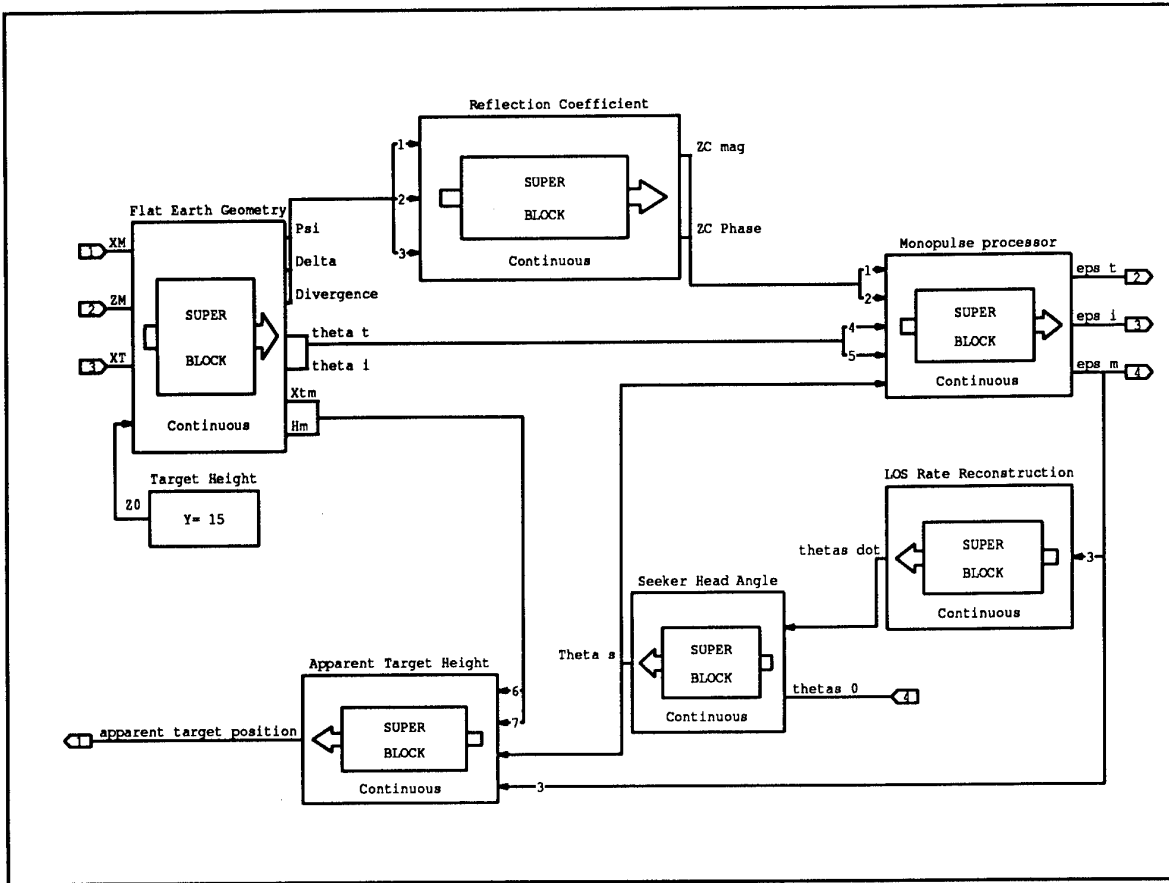


Figure 8 SystemBuild block diagram of the multipath model

Table 2 Nominal parameters for the simulated engagement

Parameter	Initial Value
Missile height	585m
Missile to target range	5400m
Missile velocity	700 m/s
Target velocity	300 m/s
Wavelength	0.03m
Dive Angle	9°
Seeker lookdown angle, $\theta_s$	6°
RMS noise	0.0°
RCS ratio ( $\sigma_A/\sigma_B$ )	0 dB
Time constants $T_a$ , $T_n$	0.2 sec
Time constant $T_s$	0.25 sec

by  $\rho_{ss}$ , where

$$\rho_{ss} = \rho \rho_c \quad (20)$$

and  $\rho_c$  is the coherent scattering co-efficient and has a value which varies non-linearly, being  $\approx 1$  for sea state zero and less than 0.1 for sea state three [4].

The effect of multipath returns from the target on the apparent target height, boresight error variations and the effect of sea state are presented in figures 9 to 12 and discussed below. It should be noted here that  $\epsilon_m$  and the apparent target height are intimately related.

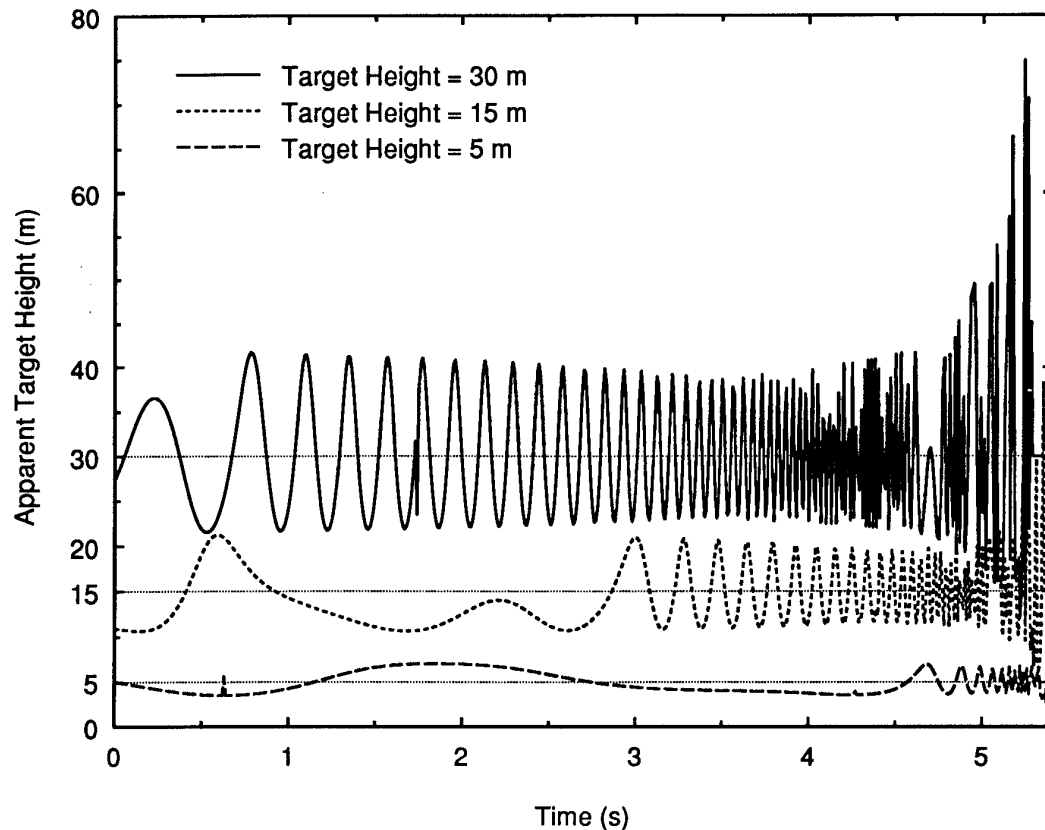


**Figure 9** Apparent target height variations for true heights of 5m, 15m and 30m for sea state zero

#### 4.1 Apparent Target Height

Figure 9 shows the apparent target height variations for true target heights of 5m, 15m and 30m and sea state zero. The time axis indicates the time from the commencement of the terminal phase and, given a closing velocity of about 1000 m/s, the range between the missile and target can be deduced using the intercept time of approximately 5.45 s. The deviation of the apparent target height from the true target height is due to multipath returns. On average, the behaviour indicates that the apparent height closely follows the true height, with multipath returns having their greatest effect in the final 2 seconds before intercept. Variations of the apparent height from the true height can be up to about 30% in each case. The frequency of the apparent target height fluctuations reflect the rate of change of the path length difference between the target and target image returns. In the final stages of the engagement, where the angular displacement between the target and image increases more rapidly (see Figure 10), the apparent height variation is seen to be the greatest. However, at no stage during the simulations did the apparent height converge towards the image height, namely, -5m, -15m and -30m, respectively. This stems directly from the magnitude of the total reflection coefficient, which, in this case is  $\approx 0.2$ , and therefore significantly reduces the strength of the target image return.

#### 4.2 Boresight error variations

Figure 10 presents the off-boresight angles, or boresight errors (BSE), to the target,  $\epsilon_t$ , the target image,  $\epsilon_i$ , and the apparent target,  $\epsilon_m$ . For each of the cases considered here, the apparent target boresight error effectively follows the target boresight error. As for the apparent target height, the deviation of  $\epsilon_m$  from  $\epsilon_t$  is due to multipath returns, and the frequency of the variation is

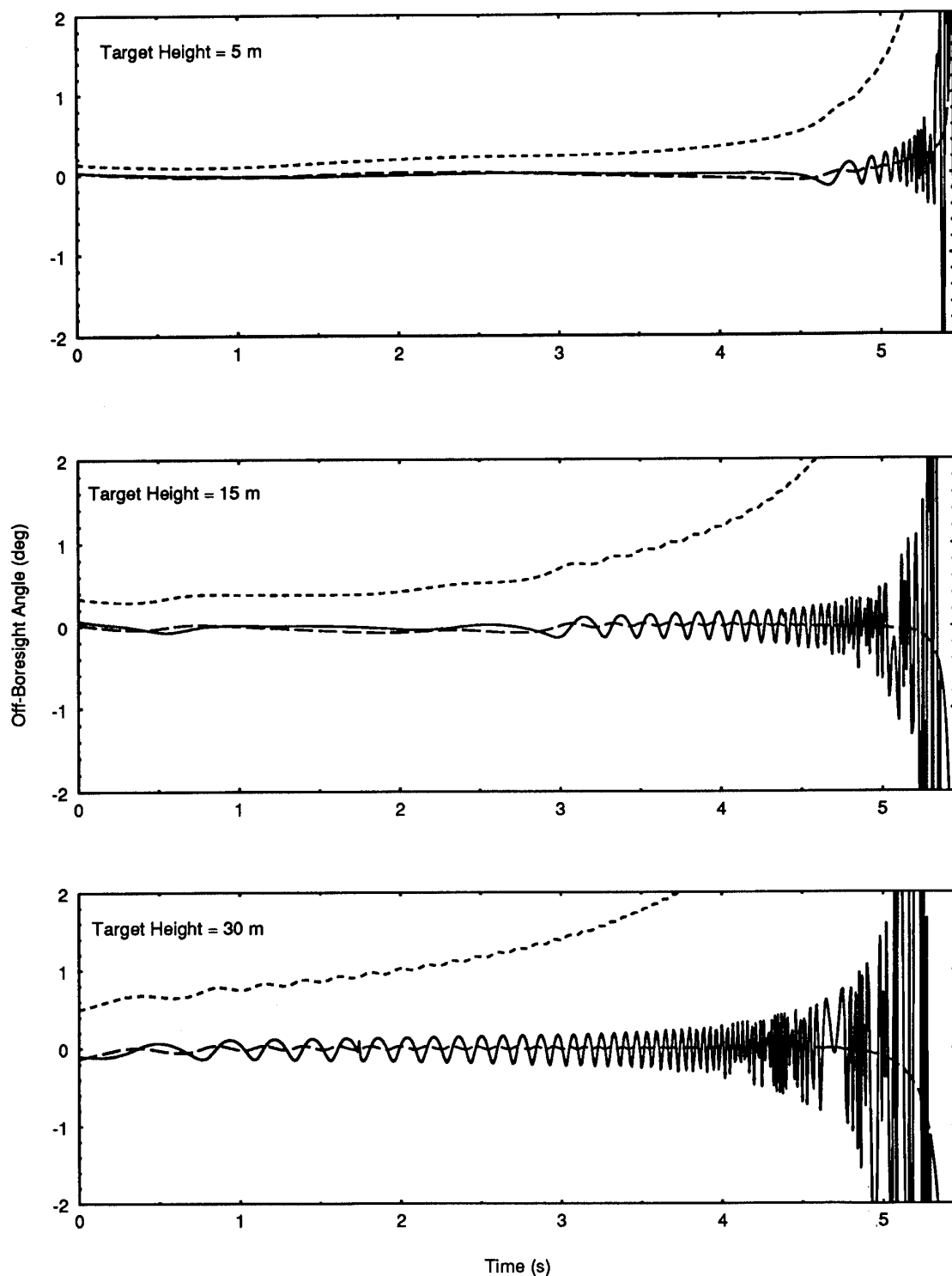


**Figure 10** The apparent target boresight error (—), the true target boresight error (— —), and the target image boresight error (---) for target heights of 5m, 15m and 30m and sea state zero

again due to the rate of change of the path length difference between the target and target image returns. Again, in the final stages of the engagement the variation was greatest, but on average, was still centred on the true target position. As in the apparent height consideration, at no stage did the apparent target position tend to the image position.

#### 4.3 Sea state

In considering the effect of sea state, entering through equation (20), a target height of 15m was considered, and the apparent target height variation and the relative power of the returned signal were examined for sea states zero and three as shown in Figures 11 and 12. A relative power of 0 dB corresponds to the direct target return and variations from this are due to the interference effects of the multipath returns.

The effect of sea state is clearly evident. A higher sea state reduces the coherent (specular) multipath returns and this is reflected in Figures 11 and 12. The coherent scattering coefficient,  $\rho_c$  in equation (20), has a value of  $\approx 1$  for sea state zero and reduces significantly to less than 0.1 for sea state three. Hence the observed effects.

### 5. CONCLUSIONS

In this paper we have presented a model for assessing the effect of multipath returns on semi-active missile guidance. The model may be used to assess the performance of particular semi-active radar homing missiles when operating over a sea surface. At present we have only considered coherent (specular) multipath, but the model is being extended to include diffuse multipath returns [3].

The results obtained above indicate that for the initial conditions considered as representative of a low-altitude engagement, an examination of apparent target height (and effectively apparent target boresight angle) indicates that although multipath returns are impacting on the predicted target position, average behaviour tends to the true target position. Any significant deviations from the true target position are extremely transient and are damped by the missile response time. Therefore they do not cause any adverse guidance problems for the missile.

A detailed assessment of the final intercept geometry (in terms of miss distance) is not justified with the simple missile model adopted here, as only qualitative effects were sought. A more quantitative analysis of the intercept geometry has been pursued using a six degree-of-freedom missile model with the incorporation of diffuse multipath returns (see reference [8] for a more detailed discussion).

### ACKNOWLEDGMENTS

The authors are grateful to Dr D.P. Brown and Mr C. Melino of DSTO for valuable input concerning various aspects of the multipath model presented herein.

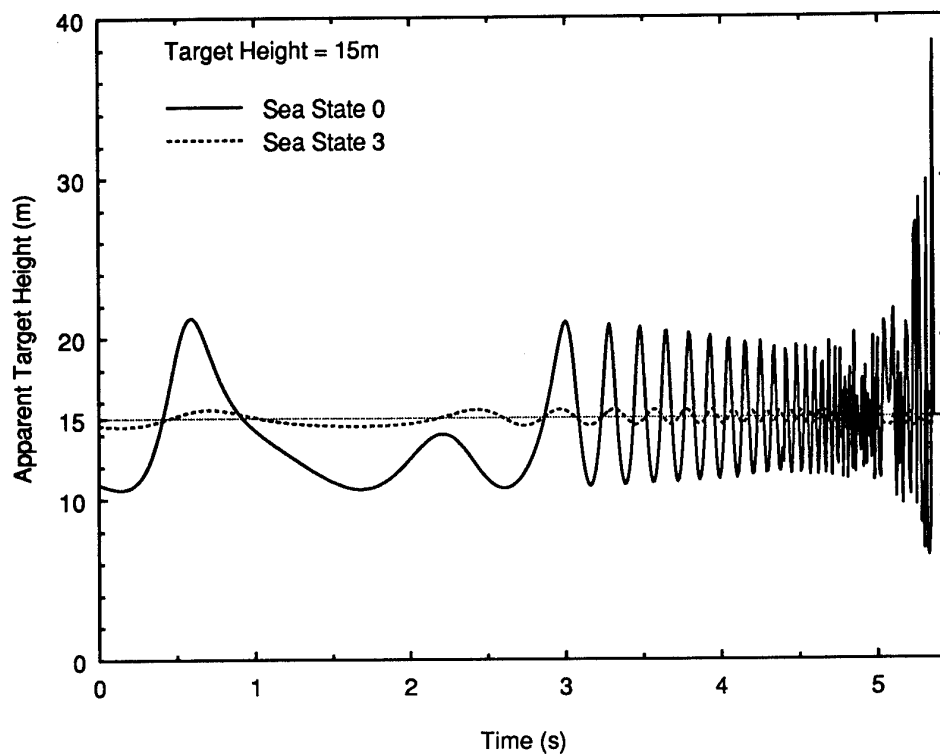


Figure 11 Effect of sea state on the apparent target height

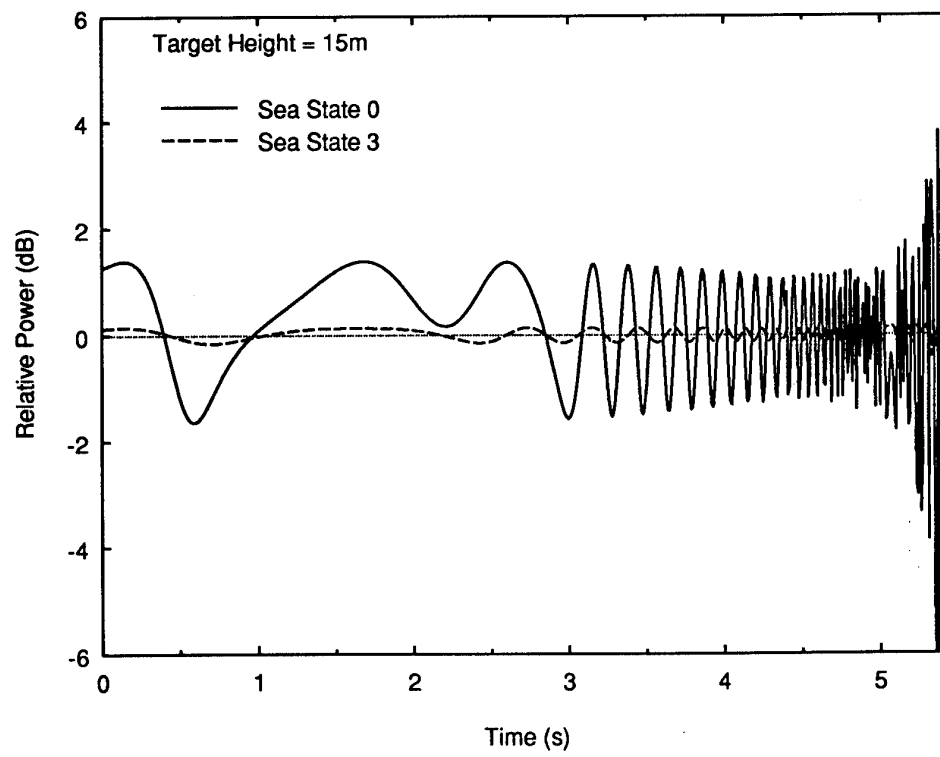


Figure 12 Effect of sea state on the relative power of the returned signal

## REFERENCES

- [1]. J.D. Hagan, NSWC White Paper: "Low elevation target multipath considerations for semi-active RF air defence missile systems", (1985). Unpublished.
- [2]. P.R. Dax, "Keep Track of that Low-Flying Attack", Microwaves, April (1976).
- [3]. D. Bucco and D. Ciampa, "A Rough Sea Multipath Model for Assessing the Performance of RF Guided Missiles against Low Altitude Targets", September (1994), (RESTRICTED). Unpublished Working Paper.
- [4]. L.V. Blake, *Radar Range-Performance Analysis*, Artech House, Norwood, MA, (1986).
- [5]. S.M. Sherman, *Monopulse Principles and Techniques*, Artech House, Norwood, MA, (1984).
- [6]. F.W. Nesline and P. Zarchan, "Line-of-sight reconstruction for faster homing guidance", *J. Guidance*, Vol. 8, No. 1, Jan-Feb (1985), pp. 3-8.
- [7]. ——, "Parametric Investigation of Standard Missile Performance Against Low Altitude Targets", Fleet Systems Department, The Johns Hopkins University, Applied Physics Laboratory, FS-86-166R (RANSI), January (1991) (Sanitised for RAN) (SECRET).
- [8]. D. Bucco, D. Ciampa and G. Ibal, "A Miss Distance Study of SM-1 Performance against Low-Altitude Targets", ERL-0809-RR, December (1994), (CONFIDENTIAL).

## DISTRIBUTION

	Copy No.
<b>Defence Science and Technology Organisation</b>	
Chief Defence Scientist	)
Central Office Executive	)
Counsellor, Defence Science, London	1 shared copy
Counsellor, Defence Science, Washington	Copy Doc Cont Data Sht
Senior Defence Scientific Adviser	Copy Doc Cont Data Sht
Scientific Adviser, POLCOM	1 copy
Navy Scientific Adviser	1 copy
Air Force Scientific Adviser	1 copy
Scientific Adviser, Army	1 copy
Assistant Secretary Scientific Analysis	1 copy
<b>Aeronautical and Maritime Research Laboratory</b>	
Director	1 copy
Chief, Weapons Systems Division	1 copy
Chiefs of other Divisions	Copy Doc Cont Data Sht
Research Leader Maritime Weapons Systems,	1 copy
Head of Missile Systems Analysis,	1 copy
Head of Radio Frequency Seekers,	1 copy
Dr D. Bucco	1 copy
Dr D. Ciampa	1 copy
Dr G. Ibal	1 copy
Dr P. Simms	1 copy
<b>Electronics and Surveillance Research Laboratory</b>	
Chief, Electronic Warfare Division	1 copy
C. Melino	1 copy
<b>Libraries and Information Services</b>	
Defence Central Library, Technical Reports Centre	1 copy
Manager, Document Exchange Centre, (for retention)	1 copy
Defence Research Information Centre, United Kingdom	1 copy
National Technical Information Service, United States	1 copy
Director Scientific Information Services, Canada	1 copy
Ministry of Defence, New Zealand	1 copy
National Library of Australia	1 copy
Defence Science and Technology Organisation Salisbury, Research Library	2 copies
Library Defence Signals Directorate Canberra	1 copy

AGPS	1 copy
British Library Document Supply Centre	1 copy
Parliamentary Library of South Australia	1 copy
The State Library of South Australia	1 copy

**Spares**

Defence Science and Technology Organisation Salisbury, Research Library	6 copies
---	----------

## DOCUMENT CONTROL DATA SHEET

Page Classification UNCLASSIFIED
Privacy Marking/Caveat N/A

1a. AR Number AR-009-242	1b. Establishment Number DSTO-TR-0163	2. Document Date APRIL 1995	3. Task Number NAV93/016			
4. Title  THE PERFORMANCE OF SEMI-ACTIVE RADAR GUIDED MISSILES AGAINST SEA SKIMMING TARGETS		5. Security Classification  <table border="1" style="display: inline-table; vertical-align: middle;"><tr><td>U</td></tr></table> Document <table border="1" style="display: inline-table; vertical-align: middle;"><tr><td>U</td></tr></table> Title <table border="1" style="display: inline-table; vertical-align: middle;"><tr><td>U</td></tr></table> Abstract	U	U	U	6. No. of Pages    27  7. No of Refs.    8
U						
U						
U						
		S (Secret)    C (Conf)    R (Rest)    U (Unclass) ♦ For UNCLASSIFIED docs with a secondary distribution LIMITATION, use (L)				
8. Authors  D.CIAMPA and D. BUCCO		9. Downgrading/Delimiting Instructions  N/A				
10 a. Corporate Author and Address  Aeronautical & Maritime Research Laboratory PO Box 1500 SALISBURY SA 5108		11. Officer/Position responsible for  Security.....SOAMRL.....  Downgrading.....DAMRL.....  Approval for Release.....DAMRL.....				
10 b. Task Sponsor  DRANSWARS						
12. Secondary Release of this Document  APPROVED FOR PUBLIC RELEASE  Any enquiries outside stated limitations should be referred through DSTIC, Defence Information Services, Department of Defence, Anzac Park West, Canberra, ACT 2600.						
13 a. Deliberate Announcement  NO LIMITATION						
13 b. Casual Announcement (for citation in other documents)  <input checked="" type="checkbox"/> No Limitation  <input type="checkbox"/> Ref. by author & Doc No only						
14. DEFTEST Descriptors  MISSILE MODELS MISSILE SIMULATORS MISSILE TARGETS		15. DISCAT Subject Codes				
16. Abstract  When a radar-guided missile engages a target at low altitudes over the sea, the radar signal reflected from the target to the missile may be subject to fading owing to multipath effects. This fading can cause serious missile guidance problems. A radar multipath model has been developed in MATRIXx to evaluate the performance of monopulse semi-active missile systems against sea skimming targets. The multipath model takes into account forward scattering over a smooth sea and includes representation of the monopulse sum and difference angle processing performed by the missile receiver. Simulation results, showing the adverse effects of multipath on the seeker boresight errors, are presented for typical missile-to-target engagements.						

Page Classification
UNCLASSIFIED
Privacy Marking/Caveat
N/A

16. Abstract (CONT.)		
17. Imprint  Aeronautical & Maritime Research Laboratory PO Box 1500 SALISBURY SA 5108		
18. Document Series and Number  DSTO-TR-0163	19. Cost Code  340/408662	20. Type of Report and Period Covered  TECHNICAL REPORT
21. Computer Programs Used		
22. Established File Reference(s)  N/A		
23. Additional Information (if required)		